AIP | Applied Physics Letters

Optically tunable long wavelength infrared quantum cascade laser operated at room temperature

S. Suchalkin, S. Jung, R. Tober, M. A. Belkin, and G. Belenky

Citation: Appl. Phys. Lett. **102**, 011125 (2013); doi: 10.1063/1.4774267
View online: http://dx.doi.org/10.1063/1.4774267
View Table of Contents: http://apl.aip.org/resource/1/APPLAB/v102/i1
Published by the American Institute of Physics.

Report Documentation Page

Form Approved
OMB No. 0704-0188

1. REPORT DATE	2. REPORT TYPE	3. DATES COVERED
09 JAN 2013		**00-00-2013 to 00-00-2013**

4. TITLE AND SUBTITLE	5a. CONTRACT NUMBER
Optically tunable long wavelength infrared quantum cascade laser operated at room temperature	5b. GRANT NUMBER
	5c. PROGRAM ELEMENT NUMBER
6. AUTHOR(S)	5d. PROJECT NUMBER
	5e. TASK NUMBER
	5f. WORK UNIT NUMBER
7. PERFORMING ORGANIZATION NAME(S) AND ADDRESS(ES) **University of Texas at Austin,Department of Electrical and Computer Engineering,Austin,TX,78759**	8. PERFORMING ORGANIZATION REPORT NUMBER
9. SPONSORING/MONITORING AGENCY NAME(S) AND ADDRESS(ES)	10. SPONSOR/MONITOR'S ACRONYM(S)
	11. SPONSOR/MONITOR'S REPORT NUMBER(S)

12. DISTRIBUTION/AVAILABILITY STATEMENT
Approved for public release; distribution unlimited

13. SUPPLEMENTARY NOTES

14. ABSTRACT

15. SUBJECT TERMS

16. SECURITY CLASSIFICATION OF:			17. LIMITATION OF ABSTRACT	18. NUMBER OF PAGES	19a. NAME OF RESPONSIBLE PERSON
a. REPORT **unclassified**	b. ABSTRACT **unclassified**	c. THIS PAGE **unclassified**	**Same as Report (SAR)**	**5**	

Optically tunable long wavelength infrared quantum cascade laser operated at room temperature

S. Suchalkin,[1] S. Jung,[1] R. Tober,[2] M. A. Belkin,[3] and G. Belenky[1]
[1]*Department of Electrical and Computer Engineering, State University of New York at Stony Brook, Stony Brook, New York 11794, USA*
[2]*Department of Electrical and Computer Engineering, The University of Texas at Austin, Austin, Texas 78759, USA*
[3]*U. S. Army Research Laboratory, Adelphi, Maryland 20873, USA*

(Received 18 September 2012; accepted 19 December 2012; published online 9 January 2013)

We demonstrate rapid tuning of the emission frequency of a room-temperature mid-infrared quantum cascade laser by external optical pumping. Emission frequency tuning over 0.3 cm^{-1} (10 GHz) has been achieved for a $\lambda = 9\,\mu m$ device by optical generation of electron-hole pairs along the entire length of the laser stripe. Measurements indicate that this approach allows for rapid broadband frequency-modulation of mid-infrared quantum cascade lasers at above 300 MHz modulation frequencies. © *2013 American Institute of Physics*. [http://dx.doi.org/10.1063/1.4774267]

Rapidly tunable quantum cascade lasers (QCLs) is a key element for the recently proposed long-wavelength infrared (LWIR) frequency modulation (FM) optical data links,[1] which can have orders of magnitude higher signal-to-noise ratio compared to the amplitude-modulation (AM) systems. More specifically, the FM advantage is proportional to $(\Delta F/f)^2$ where ΔF is the range of the carrier frequency excursion in FM modulation and f is the signal data bandwidth.[1,2]

QCLs are the only semiconductor lasers that can operate continuous-wave (CW) at room temperature in LWIR. Currently, frequency-tuning of the distributed feedback (DFB) QCLs is typically achieved by temperature control over effective refractive index using pump current modulation.[3,4] The bandwidth of the current tuning for a room temperature operated device is strictly limited since high-performance CW DFB QCLs must have efficient thermal packaging that prevents excessive heating and is estimated to be well below 25 MHz.[4] A faster way to tune a cascade laser emission frequency is by Stark modulation of the optical transition energy either within the laser active region[5–7] or in a separate passive section optically coupled with the laser waveguide.[8,9] Using the latter approach, it was possible to achieve over 10 GHz of continuous tuning of the laser emission line.[8,9] However, this approach results in a large increase in waveguide losses that prevent CW room-temperature operation of these lasers. Strong accompanying AM modulation of the laser emission[8,9] is also an undesirable effect for FM data links.

Optical excitation of electron-hole pairs in a QCL is a direct way to tune the laser wavelength through control over effective refractive index of the laser mode. It combines advantages of continuous single mode tuning and high wavelength modulation speed. Chen *et al.*[10] demonstrated 0.375 nm wavelength modulation (≈2 GHz frequency modulation) amplitude of a mid-IR QCL operated at 77 K by illuminating the QCL facet by 820 nm emission from a Ti:sapphire laser. The bandwidth of the wavelength modulation was estimated experimentally as 1.67 GHz.

In this paper, we demonstrate over 0.3 cm^{-1} (≈10 GHz) of continuous tuning with little change in the laser threshold current. We also provide direct measurements of QCL spectra and light output-current characteristics under optical excitation. To increase both tuning efficiency and pumping uniformity, we use the pumping wavelength of 1064 nm, which is in the transparency region of InP substrate and outer cladding layers in our device and is matched well to the absorption edge of the GaInAs inner waveguide cladding and the active region. The optical excitation of electron-hole pairs is achieved through the device illumination along the whole laser waveguide through the substrate for epilayer-side-down mounted devices.

The InGaAs/AlGaAs Fabry-Perot (FP) QCLs used in the experiments are based on double phonon depopulation scheme[11,12] and emitted near 9 μm at room temperature. The structure layout is shown in Figure 1(a). The lasers were processed as deep etched stripes 2 mm long and 16 μm wide. Thick (~6 μm) SU-8 2005 photoresist (MicroChem Corp.) was used as an insulation layer. The schematic of the experimental setup and the pumping geometry is presented in Figures 1(b) and 2(a). The lasers were mounted epilayer-side down onto copper blocks. Nd:YVO_3 Q-switch laser emitting at 1064 nm was used as a pumping source. Since both InP and AlInAs are transparent for this wavelength, the excitation emission was absorbed only in the active area and GaInAs inner waveguide cladding layers (Figure 2(b)). The excitation emission was coupled into the QCL through

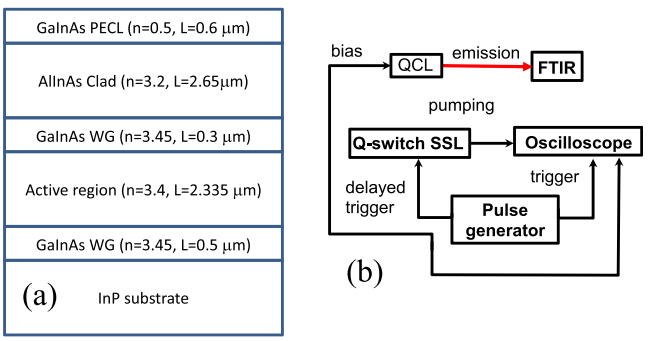

FIG. 1. (a) Quantum cascade laser waveguide layer sequence layout. (b) Schematic of the experimental setup.

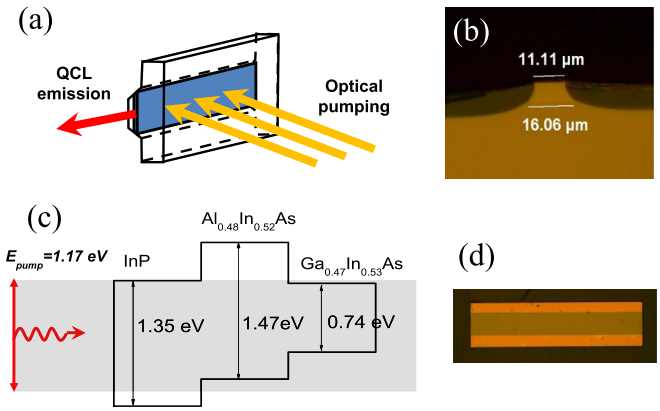

FIG. 2. (a) Optical pumping geometry used in our experiments. (b) Bandgaps of the semiconductor materials used in our device compared to the optical pumping photon energy. (c) Image of the device facet. (d) Image of the 250 μm window at the backside of our devices for optical pumping.

250 μm wide stripe window in the back contact using cylindrical optics (Figure 2(d)). QCL emission spectra were obtained using a FTIR spectrometer with resolution of 0.125 cm^{-1} and a photovoltaic MCT detector. A cylindrical lens was used to focus 1064 nm radiation into an approximately 400 μm by 2 mm spot on the laser backside. Interband photoluminescence of the QCL structure at 0.75 eV collected from the QCL front facet was used to adjust the position of the pumping beam and obtain maximum overlap between the pumping beam footprint and the QCL ridge waveguide. The Nd:YVO_3 laser produced 80 ns light pulses at 50 kHz repetition frequency. Both the 50 ns QCL bias pulse and delayed trigger pulse for the solid-state laser (SSL) were provided by the same generator (Figure 1(b)). Spectral position of a single QCL laser mode was measured at different time delays between SSL and QCL pulses.

The QCL spectrum consists of a comb of sharp peaks (laser fringes) corresponding to the different longitudinal Fabry-Perot modes. Spectral position of the peaks is determined by the effective refractive index and the cavity geometry. Due to unipolar nature of the QCL, generation of electron-hole pairs in the laser's active area does not contribute directly to the population inversion but has strong effect on the effective refractive index and, hence, on the spectral position of the laser modes.

A blue shift of the laser mode wavelength under the pumping emission was observed (Figure 3(a)). The magnitude of the shift depended continuously on the pumping power (Figure 3(b)) and reached over 0.3 cm^{-1} (≈10 GHz) at a pumping power density of only 93 W/cm^2. The frequency of one of the fringes as a function of time delay between the QCL bias and optical excitation pulses is presented in Figure 4(a). As the optical pulse of the Nd:YVO_3 laser is synchronized with the QCL bias pulse, a spectral shift of the QCL modes is observed. The signal rise and fall times shown in Figure 4(a) reflect the time resolution of the experimental setup rather than the actual photoresponse kinetics. The modal frequency shifts to the higher energy side which indicates the reduction of the effective refractive index. The change in the effective refractive index can be calculated from the spectral shift data as $\Delta n_{eff} = n_{eff}\frac{\Delta\lambda}{\lambda}$. This expression gives $\Delta n_{eff} = 1.1 \times 10^{-3}$ at the pumping density of 93 W/cm^2, using $n_{eff} \approx 3.3$ calculated for our waveguide geometry.

The spectral shift was accompanied by a decrease in QCL emission power (Figure 3(b)). Since we are working in a constant bias current mode, the drop of the laser intensity can be explained by the increase of the laser threshold due to additional optical loss caused by photo generated carriers. The light output-current characteristics of the QCL taken at different Nd:YVO_3 pumping power densities are shown in Figure 5(a). Laser threshold increase of ~9% was observed at the pumping density of 93 W/cm^2.

The change of the refractive index and increase of optical losses in our devices are resultant from electron-hole plasma created in by 1064 nm pumping both the active region and in the GaInAs inner waveguide cladding layers. Using the results of direct measurements of the QCL structure transmission and GaInAs absorption coefficient of 1.2×10^4 cm^{-1} at 1064 nm (Ref. 13), we can estimate that ≈40% of the pump power transmitted into the substrate is absorbed by the bottom InGaAs inner waveguide cladding layer, ≈30% is absorbed by the QCL active region, and ≈8% is absorbed by the top InGaAs inner waveguide cladding layer. The contributions of

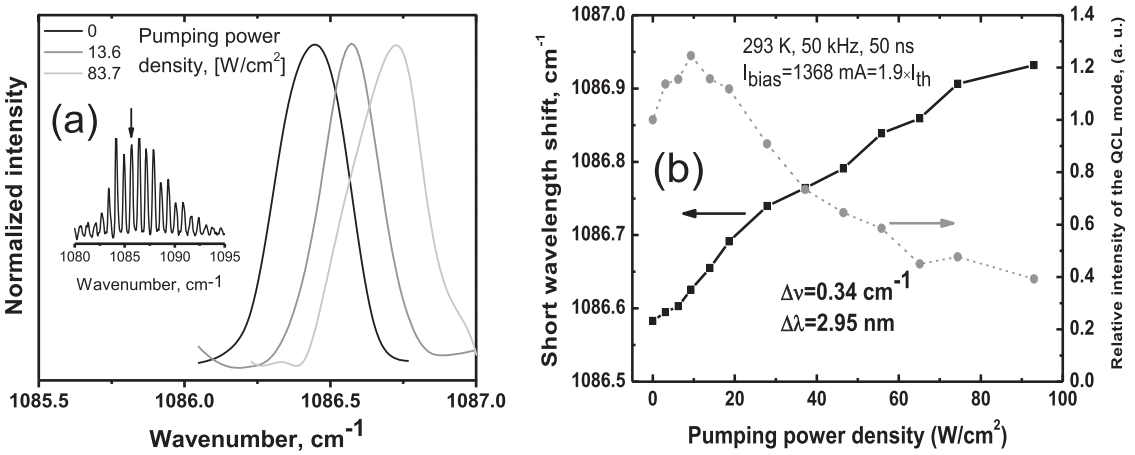

FIG. 3. (a) Zoom-in of the quantum cascade laser emission spectrum under different optical pumping intensities. A frequency shift of a single longitudinal mode is clearly seen. Inset: emission spectrum of the device. (b) Spectral position of a longitudinal mode in the QCL emission spectrum (left axis) and optical power of the mode (right axis) as a function of optical pump intensity.

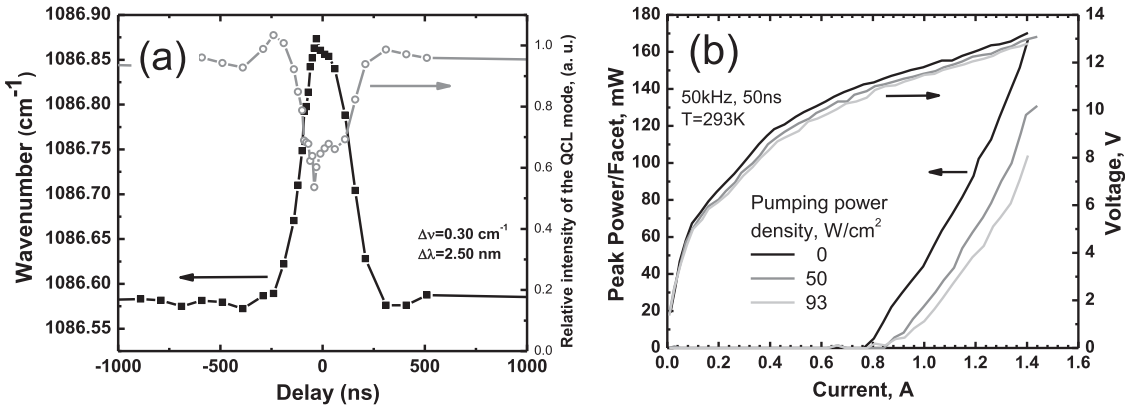

FIG. 4. (a) Spectral position of the laser mode and the power output from our device as a function of the delay of the optical pumping pulse with respect to the QCL bias pulse. (b) Light output-current (L–I) and current-voltage (I–V) characteristics of the tested device for different optical pumping intensities.

the bottom InGaAs wave guide cladding layer and the QCL active region to the change of the effective refractive index of the laser mode are commensurable. Given significantly smaller absorption in the top InGaAs cladding layer, we may neglect the contribution of this layer to the effective index change. Concentration of photo excited carriers in the active area can be roughly estimated from relative change of the current $\Delta I/I_0$ through the QCL structure under the illumination at a fixed voltage and the average doping level N_{av} of the structure: $\Delta N \approx N_{av}\frac{\Delta I}{I_0}|_{U=const}$. To do that, we used the current-voltage characteristics presented in Figure 4(b). We assumed that the major contribution to the change in the structure conductivity is given by the electrons since the transport of holes in the growth direction is almost completely blocked by the barriers. The estimation gives photo excited electron concentration of $\Delta N \approx 5 \times 10^{15}\,\mathrm{cm}^{-3}$ for the pump power of 93 W/cm^2. The contribution of photo excited carriers to the effective refractive index can be estimated using Drude model as[14]

$$\Delta n_{eff} \approx -n_0\left(\Gamma_c\frac{\Delta\omega_{pc}^2}{2\omega^2}+\Gamma_a\frac{\Delta\omega_{pa}^2}{2\omega^2}\right), \qquad (1)$$

where $\Delta\omega_{pc,pa}^2=\frac{\Delta N_{c,a}e^2}{\varepsilon_0\varepsilon m_e^*}$ is the change in the plasma frequency due to additional carrier concentrations $\Delta N_{c,a}$ in the lower inner waveguide cladding layer and active area, $\Gamma_a \approx 0.53$ and $\Gamma_c \approx 0.09$ are the confinement factors of the laser mode within the active region and within the lower InGaAs inner cladding layer, respectively, (Figure 5(a)), ω is the lasing frequency, and $n_0 \approx 3.3$ is the effective refractive index of the laser mode at zero pumping intensity. For simplicity, we further neglect the contribution to the change in n_{eff} from the lower cladding layer and focus on the contribution to Δn_{eff} from the active region only. Formula (1) is valid if $\omega_p \ll \omega$, which is the case of our experiment where $\omega \approx 2.1 \times 10^{14}$ Hz and $\omega_p \approx 1.39 \times 10^{13}$ Hz for the average doping concentration per period of $N_0 \approx 4 \times 10^{16}\,\mathrm{cm}^{-3}$. We then obtain that an additional photo excited electron concentration of $\Delta N \approx 5 \times 10^{15}\mathrm{cm}^{-3}$ in the active region produces the change of the effective refractive index of $\Delta n_{eff} \approx 0.65 \times 10^{-3}$. This value is close to the experimentally observed index variation of $\Delta n_{eff} \approx 1.1 \times 10^{-3}$ for the pump power of 93 W/cm^2. Though the contribution of free holes to the effective refractive index change, it is expected to be relatively small,[15] it may be a source for the discrepancy between experimental and theoretical values of the refractive index modulation amplitude. It should also be noted that we have omitted contributions of the cladding layers to the effective refractive index change in Eq. (1). Since the QCL lasing mode is TM polarized, to calculate free carrier contribution to the effective refractive index we have to consider polarization in the growth direction. In a first approximation, it

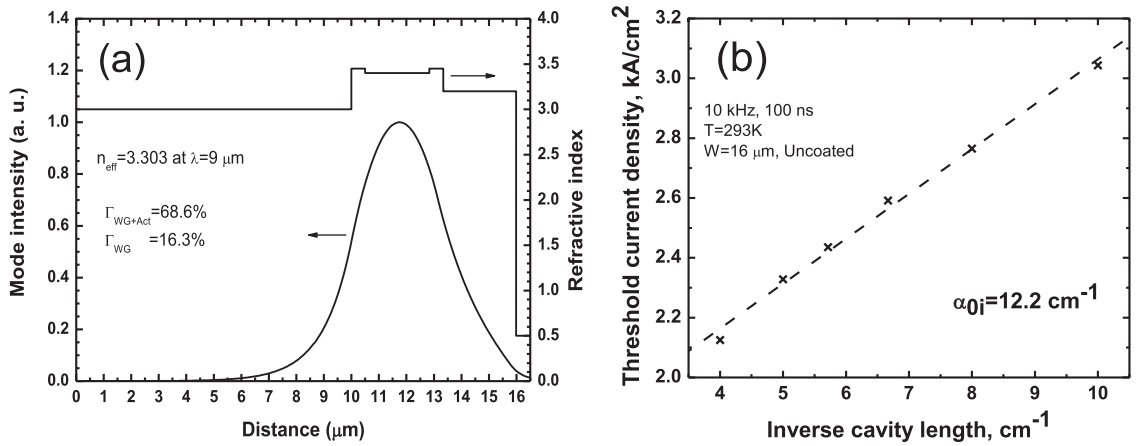

FIG. 5. (a) TM_{00} waveguide mode and waveguide refractive index profiles in our devices. (b) Dependence of the threshold current density in our devices on the reciprocal cavity length. The value of waveguide loss of $\alpha_{i0} \approx 12.2\,\mathrm{cm}^{-1}$ is obtained assuming $J_{th}(1/L) \propto \alpha_{tot} = \ln(R_m)/L + \alpha_{0i}$, where $R_m \approx 0.28$ is the uncoated facet reflectivity and L is the laser cavity length.

can be done by substituting free electron effective mass in the plasma frequency expression for corresponding parameter of the transverse motion in the injector subband. In a simple model, we can consider injector under the opening bias as a superlattice whose subband has a significant region of a quadratic spectrum near the bottom. This region is characterized by weighted average of the bulk effective masses[16] in GaInAs and AlInAs layers

$$m^*_{inj} = \frac{\tilde{d}_{GaInAs} m^*_{GaInAs} + \tilde{d}_{AlInAs} m^*_{AlInAs}}{\tilde{d}_{GaInAs} + \tilde{d}_{AlInAs}} \approx 0.054\, m_0,$$

where $\tilde{d}_{GaInAs}$ and $\tilde{d}_{AlInAs}$ are average thicknesses of GaInAs and AlInAs layers in the injector.

The additional optical loss due to the photogenerated carriers can be estimated using the relative change of the laser threshold and value of the waveguide loss in our devices $\alpha_{0i} \approx 12.2\,\mathrm{cm}^{-1}$ obtained from the experimental dependence of the reciprocal efficiency on the laser cavity length (Figure 5(b)). The main component of the waveguide loss in long wave infrared QCLs is free carrier absorption[17] whose magnitude is proportional to the carrier concentration.[14] So, additional loss $\Delta\alpha_I$ due to photo generated carriers can be estimated as

$$\Delta\alpha_i \approx \alpha_{0i} \frac{\Delta N}{N_0} = 1.5\,\mathrm{cm}^{-1}. \quad (2)$$

This value of $\Delta\alpha_I$ results in an approximately 8% increase of the total optical loss in our devices $\alpha_{tot} \approx 18.2\,\mathrm{cm}^{-1}$ (which includes mirror loss $\alpha_m \approx 6\,\mathrm{cm}^{-1}$). This number is in good agreement with the observed approximately 9% increase of the threshold current.

Lifetime of the photo excited carries in the active region can be estimated as

$$\tau \approx \frac{\Delta N h\nu_{NIR} d}{P} \approx 2.9\,\mathrm{ns}, \quad (3)$$

where $P \approx 65\,\mathrm{W/cm}^2$ is the absorbed pumping power, $\Delta N \approx 5 \times 10^{15}\mathrm{cm}^{-3}$ is the concentration of photo generated carriers, and d is the width of the active region. This relatively short lifetime can be explained by contribution of the surface recombination at the edge of a narrow stripe, whose width is much less than the typical carrier diffusion length ($\approx 10\,\mu$m). Since the carrier lifetime provides fundamental limitation to the optical tuning speed, the optical modulation bandwidth of the QCL wavelength is expected to be in the above 0.3 GHz which is in agreement with the results presented in Ref. 10.

In conclusion, we demonstrated optically tunable room temperature operated QCL emitting near $\lambda = 9\,\mu$m. Using optimized wavelength of the optical pumping source, we have increased pumping efficiency and demonstrated continuous QCL frequency tuning over $0.3\,\mathrm{cm}^{-1}$ (10 GHz). Given the carrier lifetime of $\tau \approx 2.9$ ns, we estimate the wavelength modulation bandwidth at above 0.3 GHz. The index change and additional absorption induced by optically generated free carriers are described well within the Drude model.

We wish to thank Professor B. Laikhtman for stimulating discussions. This work was supported by National Science Foundation Grant Nos. ECCS 1028435 and ECCS 1028473.

[1]S. Luryi and M. Gouzman, Int. J. High Speed Electron. Syst. **16**(2), 559 (2006).
[2]R. R. Hayes, Appl. Opt. **40**(35), 6445–6465 (2001).
[3]A. A. Kosterev, A. L. Malinovsky, F. K. Tittel, C. Gmachl, F. Capasso, D. L. Sivco, J. N. Baillargeon, A. L. Hutchinson, and A. Y. Cho, Appl. Opt. **40**(30), 5522–5529 (2001).
[4]T. Beyer, M. Braun, and A. Lambrecht, J. Appl. Phys. **93**(6), 3158–3160 (2003).
[5]A. Bismuto, R. Terazzi, M. Beck, and J. Faist, Appl. Phys. Lett. **96**(14), 141105 (2010).
[6]Y. Yao, Z. J. Liu, A. J. Hoffman, K. J. Franz, and C. F. Gmachl, IEEE J. Quantum Electron. **45**(5–6), 730–736 (2009).
[7]S. Suchalkin, M. V. Kisin, S. Luryi, G. Belenky, F. J. Towner, J. D. Bruno, C. Monroy, and R. L. Tober, Appl. Phys. Lett. **88**(3), 031103 (2006).
[8]J. Teissier, S. Laurent, C. Manquest, C. Sirtori, A. Bousseksou, J. R. Coudevylle, R. Colombelli, G. Beaudoin, and I. Sagnes, Opt. Express **20**(2), 1172–1183 (2012).
[9]M. Kisin, S. Suchalkin, and G. Belenky, IEEE Photon. Technol. Lett. **19**(5–8), 426 (2007); M. Jang, S. Suchalkin, and M. A. Belkin, IEEE J. Quantum Electron **49**(1), 60 (2013).
[10]G. Chen, R. Martini, S. W. Park, C. G. Bethea, I. C. A. Chen, P. D. Grant, R. Dudek, and H. C. Liu, Appl. Phys. Lett. **97**(1), 011102 (2010).
[11]J. Faist, D. Hofstetter, M. Beck, T. Aellen, M. Rochat, and S. Blaser, IEEE J. Quantum Electron. **38**(6), 533–546 (2002).
[12]M. A. Stroscio, M. Kisin, G. Belenky, and S. Luryi, Appl. Phys. Lett. **75**(21), 3258–3260 (1999).
[13]M. S. Alam, M. S. Rahman, M. R. Islam, A. G. Bhuiyan, and M. Yamada, presented at the IEEE 19th International Conference on Indium Phosphide & Related Materials, IPRM '07, 2007.
[14]C. A. Evans, D. Indjin, Z. Ikonic, and P. Harrison, J. Comput. Electron. **11**(1), 137–143 (2012).
[15]P. P. Paskov, J. Appl. Phys. **81**(4), 1890–1898 (1997).
[16]S. Suchalkin, G. Belenky, S. P. Svensson, B. Laikhtman, D. Smirnov, L. C. Tung, and S. Bandara, J. Appl. Phys. **110**(4), 043720 (2011).
[17]C. Sirtori, P. Kruck, S. Barbieri, H. Page, J. Nagle, M. Beck, J. Faist, and U. Oesterle, Appl. Phys. Lett. **75**(25), 3911–3913 (1999).